Supplementary information for

Optimal light harvesting in 2D semiconductor heterostructures

Zhesheng Chen [1,2,3], *Johan Biscaras*[1], *and Abhay Shukla* [1]

1 Institut Institut de Minéralogie, de Physique des Matériaux et de Cosmochimie, Sorbonne Universités - UPMC Univ Paris 06, CNRS-UMR7590, 4 Place Jussieu, Paris 75252, France

2 Laboratoire des Solides Irradiés, Ecole polytechnique, Université Paris Saclay, 91128 Palaiseau cedex, France

3 School of Nuclear Science and Technology, Lanzhou University, Lanzhou 730000, P.R. China

Email address zheshengchen@gmail.com and abhay.shukla@upmc.fr

1 Adhesion comparison of samples fabricated under different temperatures

In the traditional mechanical exfoliation experiment, 2D precursors (flakes cleaved from bulk material) were firstly cleaved by special adhesive tape, then the adhesive tape with the 2D precursors stuck on it was mechanically pressed on the desired substrates, which leaves some ultra-thin layers of 2D materials. We have introduced the parameter of temperature control and further improved this method. In our experiment, firstly, the substrates are heated at a certain temperature on a hot plate. Secondly, the precursors are exfoliated several times by adhesive tape. Thirdly, the adhesive tape containing precursors is pressed on the substrates and then peeled off. Finally monolayer or few-layer samples are identified by optical microscopy. The

comparisons of adhesion of MoS_2 and InSe fabricated under different temperatures are shown in Figure S1 and Figure S2 respectively.

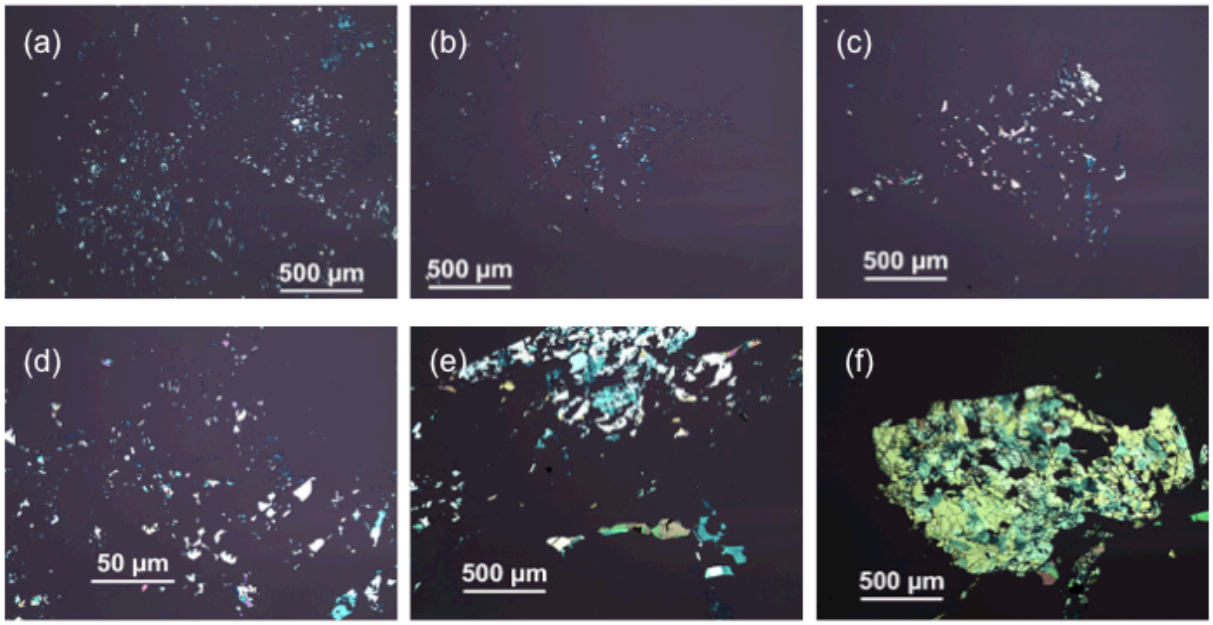

Figure S1 Comparison of optical images of few-layer InSe in large scale with different temperature prepared on SiO_2/Si substrate. (a) Room temperature (b) 50 ºC (c) 75 ºC (d) 100 ºC (e) 125 ºC and (f) 150 ºC.

For few-layer InSe preparation, at room temperature, some small flakes were left on the substrate which indicates poor sticking between the precursor and the substrate. In this case, there are some few-layer InSe samples but the sizes are less than 10 µm. When the temperature is increased to between 50 ºC and 75 ºC, the sizes of flakes increases, which means sticking is improved by the enhancement of temperature. When the temperature is between 100 ºC to 125 ºC the flake size on the substrate increases further with larger few-layer InSe flakes. This is the optimum temperature for few-layer InSe since for temperatures up to 150 ºC the flakes on the substrate become very thick and the adhesive tape leaves residues. For few-layer MoS_2

preparation, the results are also identical with an optimal substrate temperature of between 100 ºC and 125 ºC by the mechanical exfoliation method.

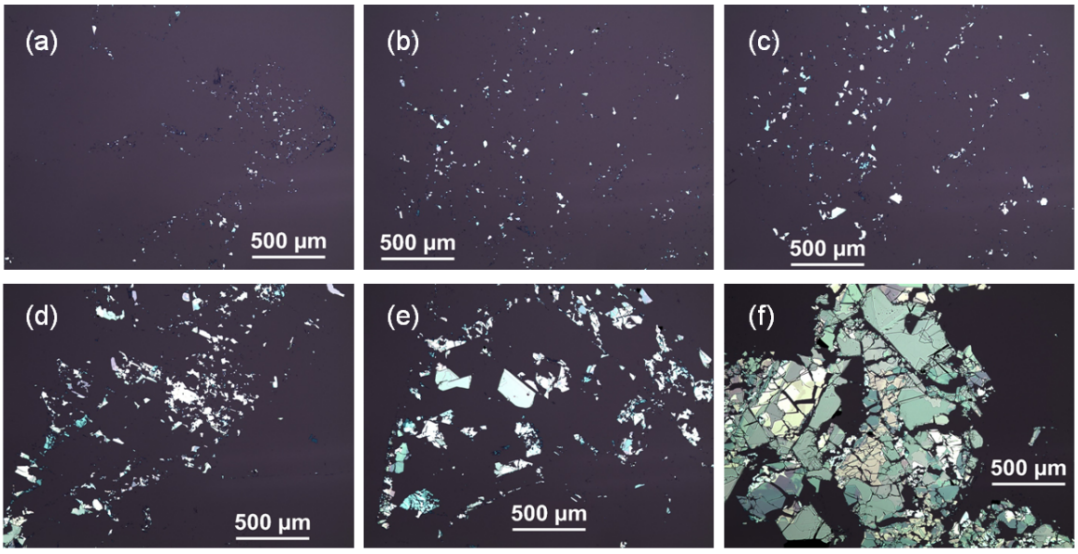

Figure S2 Comparison of optical images of few-layer MoS_2 in large scale with different temperature prepared on SiO_2/Si substrate. (a) Room temperature (b) 50 ºC (c) 75 ºC (d) 100 ºC (e) 125 ºC (f) 150 ºC.

2 High yield and clean surface of 2D semiconductor-heterostructure fabricated by random transfer method

Here we take one example of InSe/MoS_2 heterostructure to show the high yield and clean surface of 2D semiconductor-heterostructure fabricated by our random transfer method. The fabrication process is shown in Figure S3(a-c). Firstly, we mechanically exfoliate InSe onto the clean SiO_2/Si substrate at 110 ºC (patterned gold crosses are useful for referencing interesting areas). Secondly (Figure S3(C)), few-layer MoS_2 is mechanically exfoliated onto InSe/SiO_2/Si substrate at the same temperature. One can find tens of overlapping areas corresponding to InSe/MoS_2 heterostructures by using optical microscopy after this step. We show three such representative

areas and check the surface quality by using AFM. From the optical images, the sizes of InSe/MoS_2 heterostructures are 10~20 μm, which are enough to investigate light scattering by using focused Raman microscopy (focused spot: ~1 μm). AFM mapping reveals clean surfaces without bubbles or chemical residues. The thicknesses of these heterostructures are InSe (29.1 nm)/MoS_2 (27.1 nm), InSe (43.7 nm)/MoS_2 (14.6 nm), InSe (26.6 nm)/MoS_2 (14.6 nm) and InSe (55.5 nm)/MoS_2 (12.2 nm) respectively.

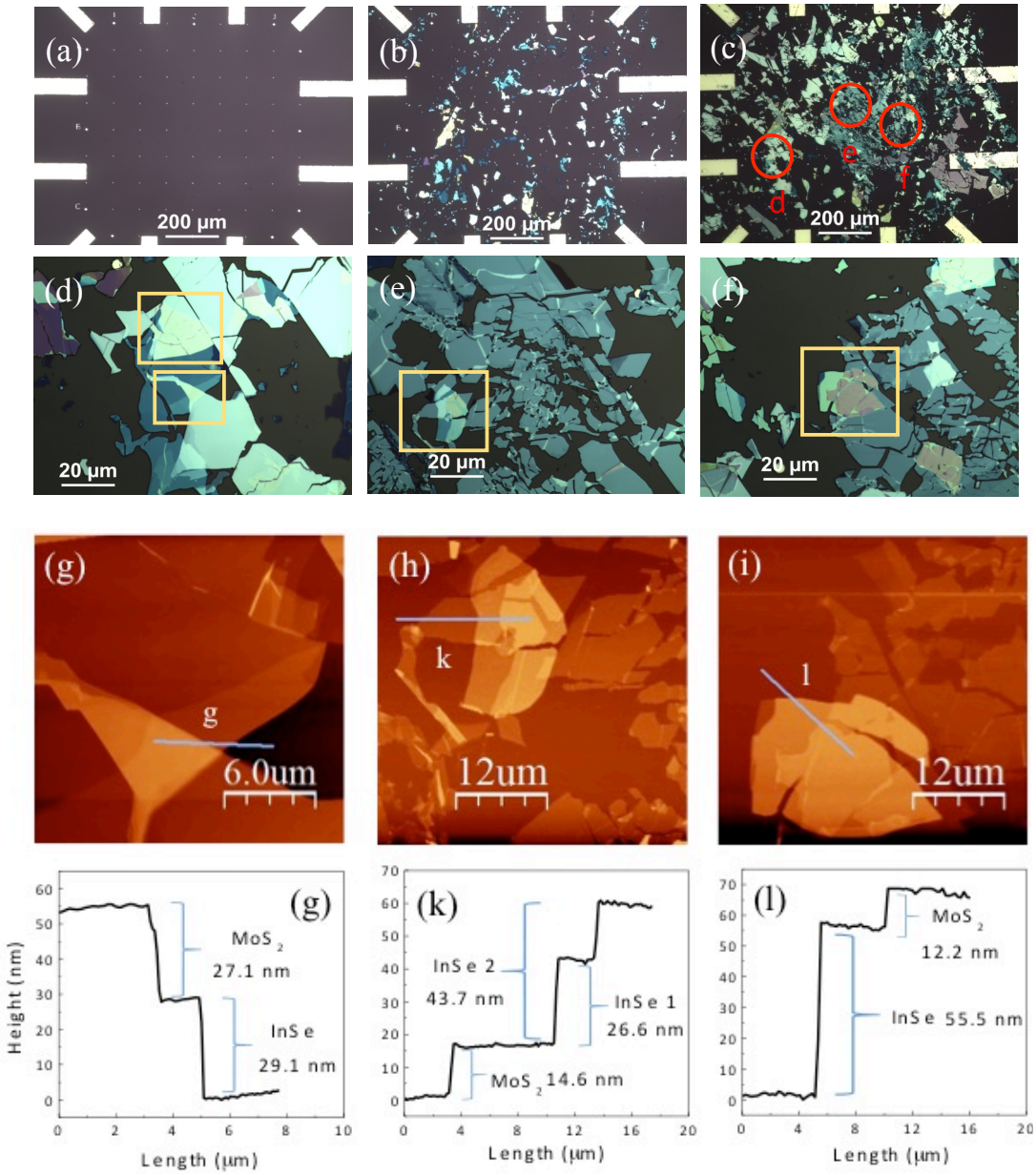

Figure S3 Fabrication process of InSe/MoS_2 heterostructure and the corresponding AFM. (a) SiO_2/Si substrate. (b) First step: mechanical exfoliation of MoS_2 at 110 ºC. (c) Second step: mechanical exfoliation of InSe at 110 ºC, examples of overlapping heterostructure areas labeled by red circles correspond to the optical images of (d-f). (g-l) the corresponding AFM of the heterostructure areas.

3 Calculation of light interaction in semiconductor-1/semiconductor-2 heterostructure

The Raman enhancement or attenuation in 2D semiconductors according to the wavelength used and the thickness of 2D samples were calculated by M. Buscema *et al*. and others [S1-S3]. Here, We present the derivation of the similar optical interference model for semiconductor-1/semiconductor-2 van der Waals heterostructure prepared on SiO_2 (285 nm)/Si substrate shown in Figure S4. There are five media including air, semiconductor-1, semiconductor-2, SiO_2 and Si which are labeled as 0, 1, 2, 3 and 4 respectively.

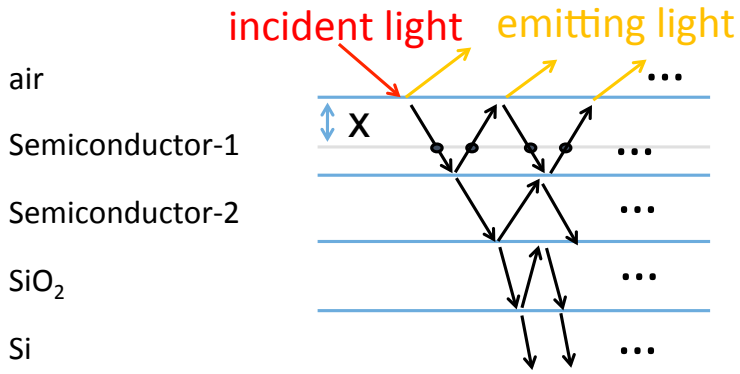

Figure S4. Schematic ray diagram of the semiconductor-1/semiconductor-2 heterostructure prepared on SiO_2/Si substrate, including multiple reflections at every interface and absorption and emission at a depth X in the semiconduction-1 layer.

Each layer has a complex index of refraction: $N_i = n_i - ik_i$ where n_i and k_i are the real and imaginary parts of the complex refraction index of layer i (i= 0, 1, 2, 3 or 4). The refractive indices of InSe, MoS_2, SiO_2 and Si we used during the calculation are given in Figure S5 [S4-S7]. The refractive indices corresponding to $A^1{}_{1g}$ Raman mode of InSe and $E^1{}_{2g}$ Raman mode of MoS_2 are listed in **Table S1**. The Fresnel reflection (r_{ij}) and transmission (t_{ij}) coefficients for a

light travelling from medium *i* to medium *j* and impinging on the *ij* interface are described as follows:

$$r_{ij} = \frac{N_i - N_j}{N_i + N_j} \quad (1)$$

$$t_{ij} = \frac{2N_i}{N_i + N_j} \quad (2)$$

From the description, one can get the relations: $r_{ij} = -r_{ji}$ and $t_{ij}t_{ji} - r_{ij}r_{ji} = 1$.

The depth dependent phase can be defined as: $\beta_i = 2\pi N_i \frac{d_i}{\lambda}$ with $n \geq 1$. For example, at a point *x* in the depth of semiconductor-1 layer, the phase difference can be defined as $\beta_x = 2\pi N_1 \frac{x}{\lambda}$.

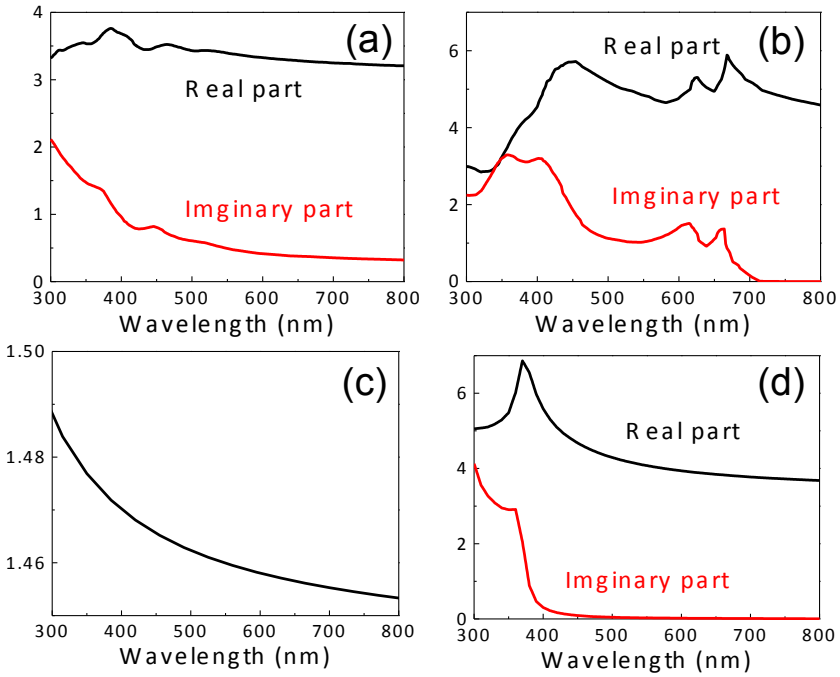

Figure S5. The refractiveindex of (a) InSe, (b) MoS_2, (c) SiO_2 and (d) Si used in our calculations.

Table S1. A list of refractive indices used for calculating the A^1_{1g} Raman mode of InSe and E^1_{2g} Raman mode of MoS_2 (Adopted from Refs. S4-S8).

Vibration mode	Raman shift	Wavelength	Air	InSe	MoS_2	SiO_2	Si
MoS_2 excited by 532 nm (E_{2g}^1 mode)	-	532 nm	1	3.43-0.54i	4.96-1.03i	1.461	4.14-0.03i
	382.5 cm^{-1}	543.05 nm	1	3.41-0.51i	4.88-1.02i	1.460	4.10-0.03i
InSe excited by 532 nm (A_{1g}^1 mode)	-	532 nm	1	3.43-0.54i	4.96-1.03i	1.461	4.10-0.03i
	114.5 cm^{-1}	535.26 nm	1	3.42-0.53i	4.94-1.03i	1.461	4.13-0.03i
InSe excited by 638 nm (A_{1g}^1 mode)	-	638 nm	1	3.29-0.38i	5.06-0.93i	1.457	3.86-0.02i
	114.5 cm^{-1}	642.69 nm	1	3.29-0.38i	5.00-0.98i	1.457	3.86-0.02i

Firstly, we calculate the effective reflection coefficient at the semiconductor-2/SiO_2 (direction: from semiconductor-2 to SiO_2) interface shown in Figure S5(a), each component (r_i) is defined as

$$r_1 = r_{23} \tag{3}$$

$$r_2 = t_{23}e^{-i\beta_3} \cdot t_{34}e^{-i\beta_3} \cdot t_{32} = t_{23}t_{32}r_{34}e^{-2i\beta_3} \tag{4}$$

$$r_3 = t_{23}e^{-i\beta_3} \cdot r_{34}e^{-i\beta_3} \cdot r_{32}e^{-i\beta_3} \cdot r_{34}e^{-i\beta_3} \cdot t_{32} = r_2(r_{32}r_{34}e^{-2i\beta_3})^1 \tag{5}$$

…

$$r_n = r_2(r_{32}r_{34}e^{-2i\beta_3})^{n-2} \tag{6}$$

The total reflection (r') is the sum over all r_n and, taking into account the relationships between the transmission and reflection coefficients expressed before, it can be reduced as:

$$r' = \frac{r_{23}+r_{34}e^{-2i\beta_3}}{1+r_{23}r_{34}e^{-2i\beta_3}} \tag{7}$$

Secondly, the same calculation can now be applied to the interface of semiconductor-1/semiconductor-2 (direction: from semiconductor-1 to semiconductor-2) shown in Figure S5(b). The total reflection r'' can be reduced as:

$$r'' = \frac{r_{12}+r'e^{-2i\beta_2}}{1+r_{12}r'e^{-2i\beta_2}} \tag{8}$$

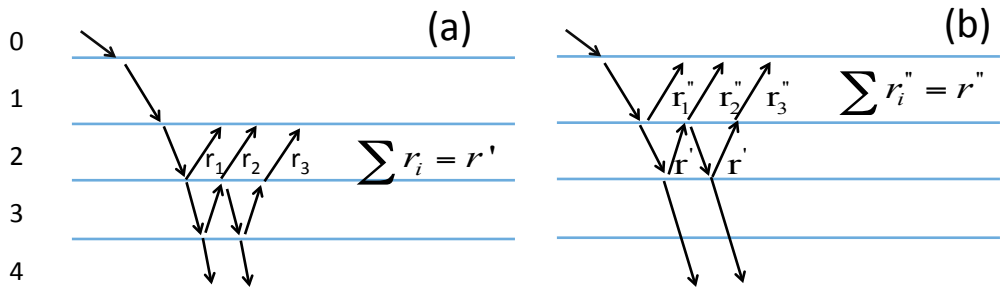

Figure S5. The total reflection r' in the semiconductor-2/SiO_2 interface (direction: from semiconductor-2 to SiO_2) and r'' in the semiconductor1/semiconductor-2 interface (direction: from semiconductor-1 to direction: from semiconductor-2).

By using the same step, we calculated the total reflection in the semiconductor-1/ semiconductor-2 interface r''' (direction: from semiconductor-2 to semiconductor-1) and the total refraction in the semiconductor-1/semiconductor-2 interface t''' (direction: from semiconductor-1 to semiconductor-2), respectively.

$$r''' = r_{21} + \frac{t_{12}t_{21}r_{10}e^{-2i\beta_1}}{1 - r_{10}r_{12}e^{-2i\beta_1}} \quad (9)$$

$$t''' = \frac{t_{10}t_{21}e^{-2i\beta_1}}{1 - r_{10}r''e^{-2i\beta_1}} \quad (10)$$

3.1 Light intensity distribution in semiconductor-1/semiconductor-2 heterostructure

In the semiconductor-1/semiconductor-2 heterostructure, the light field $E_{abs}(x)$ at the depth of x of semiconductor-1 can be described by the sum of each component abs_i:

$$abs_1 = t_{01}e^{-i\beta_x} \quad (11)$$

$$abs_2 = t_{01}e^{-i\beta_1} \cdot r''e^{-i(\beta_1 - \beta_x)} = t_{01}r''e^{-i(2\beta_1 - \beta_x)} \quad (12)$$

$$abs_3 = t_{01}e^{-i\beta_1} \cdot r'' e^{-i\beta_1} \cdot r_{10}e^{-i\beta_x} = abs_1(r_{10}r'' e^{-2i\beta_1}) \tag{13}$$

$$abs_4 = t_{01}e^{-i\beta_1} \cdot r'' e^{-i\beta_1} \cdot r_{10}e^{-i\beta_1} \cdot r'' e^{-i(\beta_1-\beta_x)} = abs_2(r_{10}r'' e^{-2i\beta_1}) \tag{14}$$

...

$$abs_{2n+1} = abs_1(r_{10}r'' e^{-2i\beta_1})^n \tag{15}$$

$$abs_{2n+2} = abs_2(r_{10}r'' e^{-2i\beta_1})^n \tag{16}$$

Therefore, the light field is given by the sum over all the *n* terms $E_{abs}(x) = \sum abs_i$ and results in:

$$E_{abs}(x) = t_{01} \cdot \frac{e^{-i\beta_x} + r'' e^{-i(2\beta_1-\beta_x)}}{1 + r'' r_{01} e^{-2i\beta_1}} \tag{17}$$

The light intensity at the depth of x in semiconductor-1 is: $I(x) = \left|E_{abs}(x)\right|^2$. In the same way, the light intensity at the depth of y in semiconductor-2 is: $I(y) = \left|E_{abs}(y)\right|^2$, in which $E_{abs}(y)$ is:

$$E_{abs}(y) = \frac{t_{01}t_{12}e^{-i\beta_1}e^{-i\beta_y} + r' e^{-i(2\beta_2-\beta_y)}}{1 - r''' r' e^{-2i\beta_2}} \tag{18}$$

3.2 Light scattering from semiconductor-1/semiconductor-2 heterostructure

The light scattering process in semiconductor-1/semiconductor-2 heterostructure can be seprated into two components: light distribution and light emission resulting from this light distribution. For the light scattering from semiconductor-1 of the heterostructure, the total intensity can be written as:

$$I_{scatter} = \int_0^{d_1} \left|E_{abs}(x) \cdot E_{emi}(x)\right|^2 dx \tag{19}$$

$F_{emi}(x)$ is the light emission at the depth of x in semiconductor-1:

$$E_{emi}(x) = t_{10} \cdot \frac{e^{-i\beta_x} + r'' e^{-i(2\beta_1 - \beta_x)}}{1 + r'' r_{01} e^{-2i\beta_1}} \tag{20}$$

In the same way, for the light scattering from semiconductor-2 of the heterostructure, the total intensity can be written as:

$$I_{scatter} = \int_0^{d_2} \left| E_{abs}(y) \cdot E_{emi}(y) \right|^2 dy \tag{21}$$

$F_{emi}(y)$ is the light emission at the depth of y in semiconductor-2:

$$E_{emi}(y) = t''' \cdot \frac{e^{-i\beta_y} + r' e^{-i(2\beta_2 - \beta_y)}}{1 - r''' r' e^{-2i\beta_2}} \tag{22}$$

4 Comparison of Raman intensity enhancement or attenuation from different stacking sequenced 2D semiconductor-heterostructure

In Figure S6 we show an example of Raman intensity enhancement or attenuation in a 2D semiconductor-heterostructure by changing the stacking sequence of InSe and MoS_2 layers. For the Raman intensity of the InSe A_{1g}^1 mode under 532 nm excitation, the optimum Raman intensity is from a InSe (40 nm)/MoS_2 (25 nm) heterostructure, however when the stacking sequence is inverted the optimum intensity is from InSe (78 nm)/MoS_2 (0 nm). For the Raman enhancement factor F, the maximum value in a InSe/MoS_2 heterostructure is 6, occurring in a heterostructure of thickness 40 nm/25 nm, while the maximum is ~2 when the stacking sequence is inverted to MoS_2 (40 nm)/ InSe (25 nm).

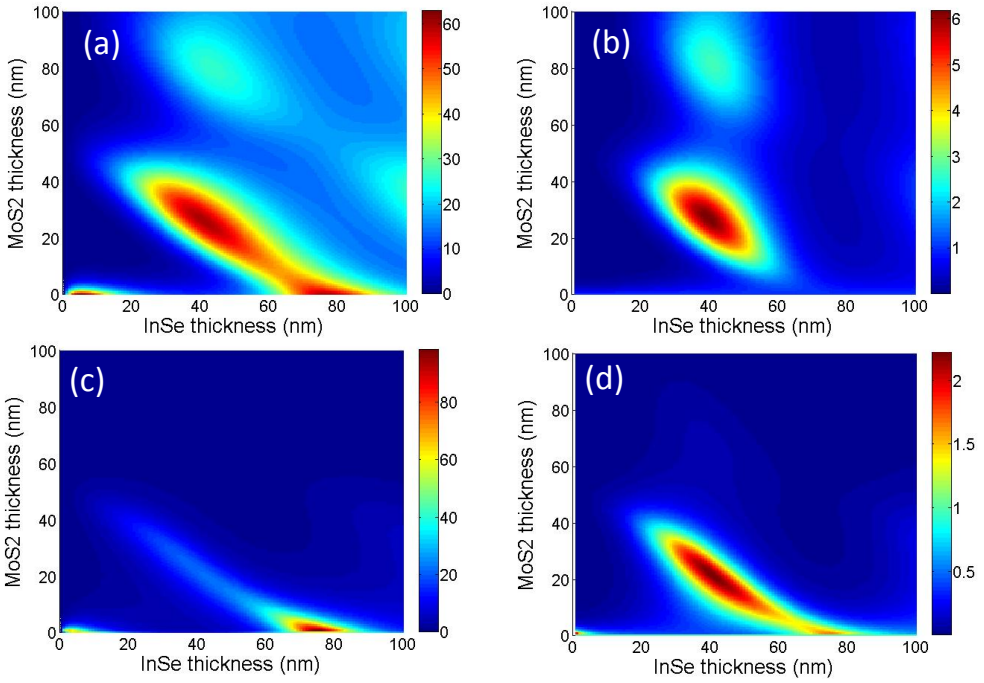

Figure S6. (a-b) Calculation of Raman intensity and enhancement factor F (InSe A_{1g}^1 mode under 532 nm excitation) in InSe/MoS_2 heterostructure. (c-d) Calculation of Raman intensity and enhancement factor F (InSe A_{1g}^1 mode under 532 nm excitation) in MoS_2/InSe heterostructure.

5 Light intensity distribution under different thickness of InSe/MoS_2 heterostructure

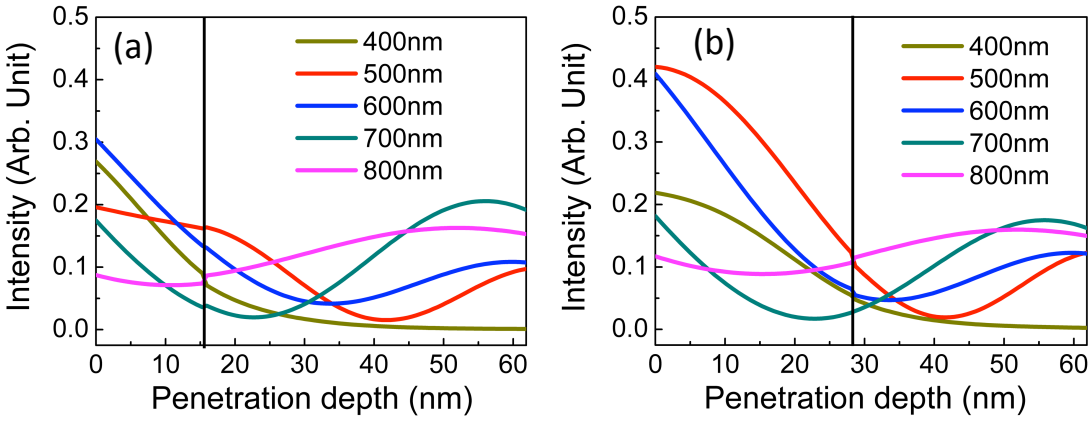

Figure S7. Light intensity distribution in (a) the InSe (28.1 nm)/MoS2 (33.9 nm) heterostructure and (b) the InSe (15.2 nm)/MoS2 (44.8 nm) heterostructure.

6 Intensity distribution of MoS_2/InSe heterostructure fabricated on SiO_2/Si substrate and glass substrate

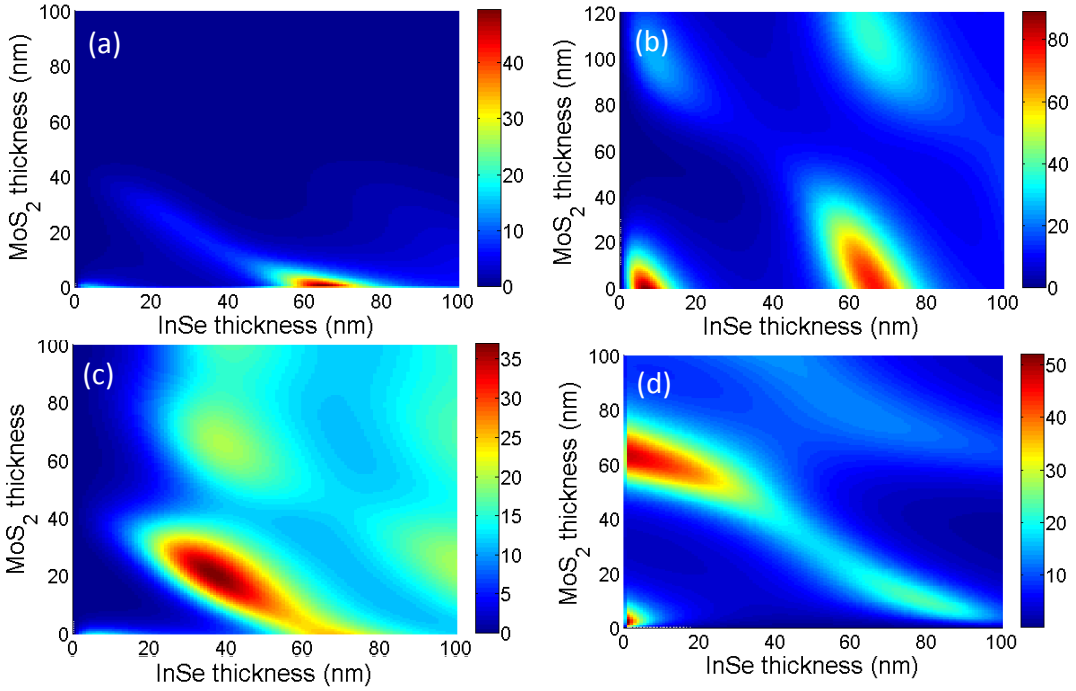

Figure S7. (a) Intensity distribution of InSe under 484 nm in MoS_2/ InSe heterostructure fabricated on SiO_2/Si substrate. (b) Intensity distribution of MoS_2 under 681 nm in MoS_2/ InSe heterostructure fabricated on SiO_2/Si substrate. (c) Intensity distribution of InSe under 484 nm in MoS_2/ InSe heterostructure fabricated on glass substrate. (d) Intensity distribution of MoS_2 under 681 nm in MoS_2/ InSe heterostructure fabricated on glass substrate.

References

[S1] Buscema, M.; Steele, G. A.; van der Zant, H. S. J.; Castellanos-Gomez, A. The effect of the substrate on the Raman and photoluminescence emission of single layer MoS_2. *Nano Res.* **2014**, **7**, 561-571.

[S2] Li, S. L.; Miyazaki, H.; Song, H.; Kuramochi, H.; Nakaharai, S.; and Tsukagoshi, K. Quantitative Raman Spectrum and Reliable Thickness Identification for Atomic Layers on Insulating Substrates. *ACS Nano* **2012**, *6*, 7381–738.

[S3] Lien, D.-H.; Kang, J. S.; Amani, M.; Chen, K.; Tosun, M.; Wang, H. P.; Roy, T.; Eggleston, M. S.; Wu, M. C.; Dubey, M.; Lee, S.-C.; He, J.-H.; Javey, A. Engineering Light Outcoupling in 2D Materials. *Nano Lett.* **2015**, *15*, 1356–1361.

[S4] Beal, A. R., Hughes, H. P. Kramers-Kronig analysis of the reflectivity spectra of 2H-MoS_2, 2H-$MoSe_2$ and 2H-$MoTe_2$, *J. Phys. C: Solid State Phys.* **1979**, *12*, 881-890.

[S5] Grasso, V., Perillo, P. Optical constants and interband transitions in the layer compound InSe. *Solid State Commun.* **1977**, *21*, 323-325.

[S6] Malitson, I. H. Interspecimen comparison of the refractive index of fused silica. *J. Opt. Soc. Am.* **1965**, *55*, 1205-1208.

[S7] Green M. A.; Keevers, M. J. Optical properties of intrinsic silicon at 300 K. *Prog. Photovolt: Res. Appl.* **1995**, *3*, 189 - 192.

[S8] Green, M. A. Self-consistent optical parameters of intrinsic silicon at 300 K including temperature coefficients. *Sol. Energ. Mat. Sol. Cells* **2008**, *92*, 1305–1310.